stability of the observed stress orientations with depth implies that there are no large down-dip changes in the relative strengths of the megathrust and other faults, despite substantial changes in temperature and pressure. This suggests that all faults in the subduction zone region have similar physical mechanisms controlling their strength.

REFERENCES AND NOTES

1. S. A. Peacock, *Science* **248**, 329–337 (1990).
2. R. H. Sibson, *Tectonophysics* **600**, 142–152 (2013).
3. P. M. Fulton *et al.*, *Science* **342**, 1214–1217 (2013).
4. R. H. Sibson, *J. Struct. Geol.* **7**, 751–754 (1985).
5. E. M. Anderson, *The Dynamics of Faulting and Dyke Formation with Application to Britain* (Oliver & Boyd, Edinburgh, 1951).
6. B. Célérier, *Rev. Geophys.* **46**, RG4001 (2008).
7. G. P. Hayes, D. J. Wald, R. L. Johnson, *J. Geophys. Res.* **117**, B01302 (2012).
8. A. Hasegawa, K. Yoshida, T. Okada, *Earth Planets Space* **63**, 703–707 (2011).
9. J. L. Hardebeck, *Geophys. Res. Lett.* **39**, L21313 (2012).
10. S. Ghimire, Y. Tanioka, *Tectonophysics* **51**, 1–13 (2011).
11. M. Pardo, D. Comte, T. Monfret, *J. S. Am. Earth Sci.* **15**, 11–22 (2002).
12. A. Kubo, E. Fukuyama, H. Kawai, K. Nonomura, *Tectonophysics* **356**, 23–48 (2002).
13. G. Ekström, M. Nettles, A. M. Dziewonski, *Phys. Earth Planet. Inter.* **200–201**, 1–9 (2012).
14. See supplementary materials on *Science* Online.
15. P. Molnar, T. Atwater, *Earth Planet. Sci. Lett.* **41**, 330–340 (1978).
16. A. Heuret, C. P. Conrad, F. Funiciello, S. Lallemand, L. Sandri, *Geophys. Res. Lett.* **39**, L05304 (2012).
17. C. H. Scholz, J. Campos, *J. Geophys. Res.* **117**, B05310 (2012).
18. S. Toda, R. S. Stein, J. Lin, *Geophys. Res. Lett.* **38**, L00G03 (2011).
19. K. Wang, Y. Hu, *J. Geophys. Res.* **111**, B06410 (2006).
20. M. E. Magee, M. D. Zoback, *Geology* **21**, 809–812 (1993).
21. R. J. Twiss, E. M. Moores, *Structural Geology* (Freeman, New York, ed. 2, 2007).
22. X. Gao, K. Wang, *Science* **345**, 1038–1041 (2014).
23. S. Husen, E. Kissling, *Geology* **29**, 847–850 (2001).
24. P. Audet, M. G. Bostock, N. I. Christensen, S. M. Peacock, *Nature* **457**, 76–78 (2009).
25. J. L. Hardebeck, A. J. Michael, *J. Geophys. Res.* **109**, B11303 (2004).
26. D. Eberhart-Phillips, M. Reyners, *Geophys. Res. Lett.* **26**, 2565–2568 (1999).

ACKNOWLEDGMENTS

I thank P. McCrory, A. Michael, R. Bürgmann, and an anonymous reviewer for constructive comments on an earlier version of this manuscript. The Japan National Research Institute for Earth Science and Disaster Prevention (NIED) moment tensor catalog is available from the NIED at www.fnet.bosai.go.jp/fnet/event/search.php. The Global CMT (GCMT) moment tensor catalog is available from the GCMT project at www.globalcmt.org/CMTsearch.html. The SLAB 1.0 subduction zone model is available from the U.S. Geological Survey at http://earthquake.usgs.gov/data/slab. The SATSI code used for stress inversion is available from the U.S. Geological Survey at http://earthquake.usgs.gov/research/software/#SATSI.

SUPPLEMENTARY MATERIALS

www.sciencemag.org/content/349/6253/1213/suppl/DC1
Materials and Methods
Figs. S1 and S2
References (*27*, *28*)

14 May 2015; accepted 15 July 2015
10.1126/science.aac5625

NEURONAL IDENTITY

Tuning of fast-spiking interneuron properties by an activity-dependent transcriptional switch

Nathalie Dehorter,[1,2] Gabriele Ciceri,[2]* Giorgia Bartolini,[1,2] Lynette Lim,[1,2] Isabel del Pino,[1,2]† Oscar Marín[1,2]‡

The function of neural circuits depends on the generation of specific classes of neurons. Neural identity is typically established near the time when neurons exit the cell cycle to become postmitotic cells, and it is generally accepted that, once the identity of a neuron has been established, its fate is maintained throughout life. Here, we show that network activity dynamically modulates the properties of fast-spiking (FS) interneurons through the postmitotic expression of the transcriptional regulator Er81. In the adult cortex, Er81 protein levels define a spectrum of FS basket cells with different properties, whose relative proportions are, however, continuously adjusted in response to neuronal activity. Our findings therefore suggest that interneuron properties are malleable in the adult cortex, at least to a certain extent.

Fast-spiking (FS), parvalbumin-expressing (PV^+) basket cells make up the most abundant population of GABAergic interneurons in the cerebral cortex. Although they probably represent no more than 5% of the total neuronal population, they contribute to feedback and feedforward inhibition and are critically involved in the generation of network oscillations that are crucial for sensory perception, cognition, and behavior (*1*–*5*). In addition, FS PV^+ basket cells play a prominent role in the regulation of plasticity and learning (*6*–*9*). Although it is likely that different classes of FS PV^+ interneurons exist, the molecular mechanisms regulating their properties remain largely unknown (*10*).

We previously found that neurons generated in the medial ganglionic eminence (MGE) express the transcription factor Etv1/Er81 (*11*). Because PV^+ interneurons derive from the MGE (*10*), we investigated whether Er81 is expressed in this population of interneurons. Although Er81 expression in the neocortex has been ascribed only to layer V pyramidal cells (*12*), we observed that this transcription factor is also expressed in scattered cells throughout the neocortex of postnatal mice (Fig. 1A). In layer II-III, where $Er81^+$ expressing cells are particularly abundant, the majority of these cells are PV^+ interneurons (fig. S1). Conversely, over 60% of PV^+ interneurons in layer II-III contain detectable levels of Er81 protein (Fig. 1B).

Because PV^+ interneurons in superficial layers of the cortex are heterogeneous (*13*), we wondered whether Er81 expression defines the properties of FS interneurons. We thus performed whole-cell recordings in acute slices through the primary somatosensory cortex of *PV-Cre;RCE* mice, in which PV^+ interneurons express an enhanced form of green fluorescent protein (GFP). We confirmed the identity of FS PV^+ interneurons on the basis of well-described features of their action potentials (*14*). Different classes of PV^+ FS interneurons have distinctive features in their pattern of discharge. For example, some classes of PV^+ interneurons display a prominent delay to the first spike near spike threshold potential, whereas others do not (*15*, *16*). The majority of PV^+ interneurons in layer II-III had a delayed firing pattern and expressed Er81 (n = 22/33 cells) (Fig. 1, C and E). By contrast, PV^+ interneurons with very short latency or purely nondelayed firing consistently lacked detectable levels of Er81 protein (n = 11/33 cells) (Fig. 1, D and E). Thus, although the basic membrane properties of these cells are similar (fig. S2A), Er81 expression clearly segregates two classes of PV^+ interneurons on the basis of their physiological parameters at near-threshold potential (Fig. 1, E to H). The correlation between Er81 expression and firing pattern seems universal among FS interneurons in the telencephalon. Chandelier cells, an important class of FS interneurons that exhibit nondelayed firing (*17*) (fig. S3), and the large majority of PV^+ FS cells in layer IV, which also display nondelayed features, both lack Er81 expression (fig. S4, A to D). By contrast, PV^+ interneurons in the striatum displayed a delayed firing pattern and contain Er81 (fig. S4, E to H).

To extend our observations, we analyzed the connectivity of FS interneurons in layer II-III of the somatosensory cortex. Recordings of miniature excitatory and inhibitory postsynaptic

[1]MRC Centre for Developmental Neurobiology, Medical Research Council, New Hunt's House, Guy's Campus, King's College London, London SE1 1UL, UK. [2]Instituto de Neurociencias, Consejo Superior de Investigaciones Científicas and Universidad Miguel Hernández, 03550 Sant Joan d'Alacant, Spain.
*Present address: Sloan-Kettering Institute for Cancer Research, 1275 York Avenue, New York, NY 10065, USA. †Present address: Neurocentre Magendrie, 146 rue Léo Saignat, 33077 Bordeaux cedex, France. **‡Corresponding author. E-mail: oscar.marin@kcl.ac.uk**

currents (mEPSCs and mIPSCs, respectively) revealed that Er81$^+$ FS interneurons receive significantly more excitatory synapses and far fewer inhibitory contacts than Er81$^-$ FS interneurons (Fig. 1, I to N, and fig. S2, B to G).

To determine whether Er81 plays an instructive role in the specification of delay-type FS interneurons, we specifically deleted *Er81* from the embryonic MGE by breeding *Lhx6-Cre* mice (*18*) with mice carrying loxP-flanked (F) *Er81* alleles (*19*). We observed no differences in the density and laminar distribution of PV$^+$ interneurons in the cerebral cortex of control and *Lhx6-Cre;Er81$^{F/F}$;RCE* mice at postnatal day 30 (P30) (Fig. 2A and fig. S5A), which indicated that Er81 is not required for the migration and early specification of FS interneurons. However, most FS interneurons in *Er81* conditional mutants displayed a dramatic reduction in the mean latency to the first spike, hyperpolarization of the threshold potential for spike, and a lower rheobase than control FS interneurons (Fig. 2B and fig. S5, B to D).

To assess whether Er81 function is also necessary for the maintenance of delay-type FS interneurons in the mature cortex, we generated conditional *Er81* mutant mice using *PV-Cre* mice, which only achieve effective recombination in the cortex in young adult mice (*20*). As in *Lhx6-Cre;Er81$^{F/F}$;RCE* mice, we did not observe differences in the density or distribution of PV$^+$ interneurons in the cortex of *PV-Cre;Er81$^{F/F}$;RCE* mice compared with controls at P60 (Fig. 2C and fig. S6A). However, the postnatal elimination of *Er81* also caused a prominent decrease in the mean latency to the first spike in FS interneurons from the cortex of *PV-Cre;Er81$^{F/F}$;RCE* mice (Fig. 2D and fig. S6, B to D). Because background conductance inputs may influence the relative delay in firing of the first spike, we analyzed this parameter while blocking synaptic activity. We did not observe changes in the mean latency to the first spike at threshold potential in *Er81* mutant interneurons with or without synaptic blockers (69.7 ± 19.1 ms and 60.5 ± 16.7 ms, respectively; n = 5, Student's t test, P = 0.6), which ruled out non–cell autonomous effects on these parameters.

The ability of some FS interneurons to exhibit a prominent delay of the first spike near spike threshold potential is thought to serve as an important gating mechanism of inhibitory function that is mediated by Kv1.1-containing potassium channels localized to the axon initial segment (*21*). Er81 could therefore control delayed firing in FS interneurons by regulating the expression of Kv1.1 channels. We found a prominent decrease in Kv1.1 protein levels in cortical lysates obtained from *PV-Cre;Er81$^{F/F}$;RCE* mice compared with controls (Fig. 2E). To confirm that Er81 transcriptionally controls the expression of Kv1.1 in PV$^+$ interneurons, we isolated these cells from the cortex of control and *PV-Cre;Er81$^{F/F}$;RCE* mice using fluorescence-activated cell sorting (FACS) and carried out quantitative polymerase chain reaction (PCR) analyses. We found significantly lower *Kv1.1 mRNA* levels in mutant FS interneurons than in controls (Fig. 2F). Finally, we identified ETS binding sequences upstream of the transcriptional initiation site of *Kv1.1* and demonstrated specific binding of Er81 using chromatin immunoprecipitation (ChIP) analysis in cortical lysates (Fig. 2G). Although this later experiment lacks cellular resolution, the results are consistent with the notion that Er81 regulates the intrinsic neural excitability of delay-type FS interneurons, at least in part by controlling the expression of Kv1.1 channels.

Our initial observation that delay-type and nondelay-type FS interneurons receive, on average, different number of excitatory synapses (Fig. 1, H to K) prompted us to examine the connectivity of cortical PV$^+$ interneurons in conditional *Er81* mutants. To this end, we first measured synaptic activity on FS interneurons in acute slices obtained from control and conditional *Lhx6-Cre;Er81$^{F/F}$;RCE* mice. We found a significant decrease in the frequency and amplitude of mEPSCs in mutant FS interneurons compared with control cells (Fig. 3, A to E), which suggests that loss of Er81 during development changes the inputs received by these cells. To test whether the late removal of Er81 has the same effect, we recorded synaptic activity from FS interneurons

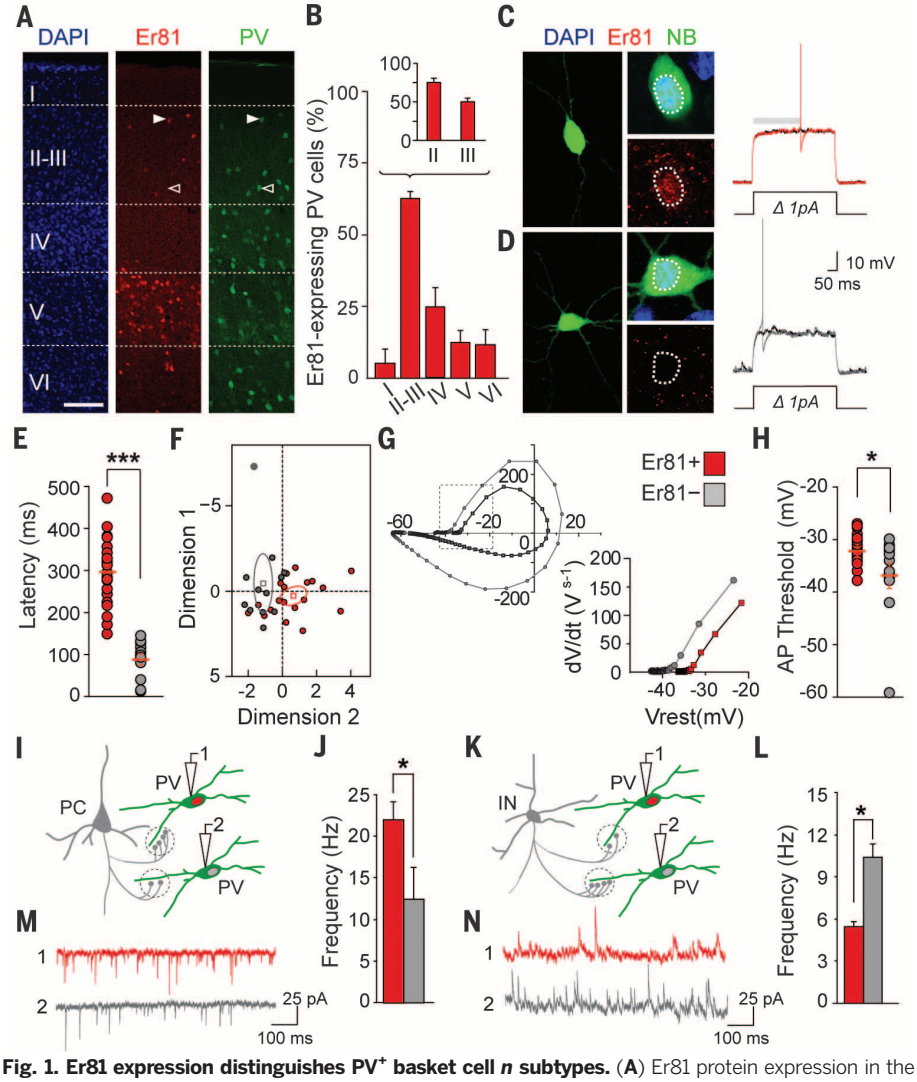

Fig. 1. Er81 expression distinguishes PV$^+$ basket cell *n* subtypes. (**A**) Er81 protein expression in the somatosensory cortex. (**B**) PV$^+$/Er81$^+$ interneurons are particularly abundant in cortical layer II-III, with a superficial to deep gradient within this layer (n = 11 P25 mice). (**C** and **D**) Representative traces of firing at near threshold potential for Er81$^+$ (red) and Er81$^-$ (gray) PV$^+$ interneurons. NB, Neurobiotin. (**E**) Mean latency to the first spike (n = 22 and 9 cells, respectively; P < 0.001). (**F**) Individual factor maps from principal component analysis performed on recorded cells reveals a significant segregation between Er81$^+$ and Er81$^-$ PV$^+$ interneurons. (**G**) Phase plane plots for Er81$^+$ and Er81$^-$ PV$^+$ interneurons. (**H**) Threshold potential for spike is significantly different between Er81$^+$ and Er81$^-$ PV$^+$ interneurons (n = 21 and 11 cells, respectively; P < 0.05). (**I** and **K**) Schematic of mEPSCs and mIPSCs recordings in PV$^+$ interneurons. PC, pyramidal cell; PV, PV$^+$ interneuron; IN, Interneuron. (**M** and **N**) Representative traces. (**J** and **L**) Measurements of mEPSC (n = 15 and 6 cells, respectively; P < 0.05) and mIPSC (n = 7 and 4 cells, respectively; P < 0.05) frequencies in PV$^+$ interneurons. Scale bars, 100 μm (A) and 10 μm (C) and (D). Graphs represent means ± SEM.

in control and *PV-Cre;Er81*$^{F/F}$*;RCE* mice. We found a significant decrease in the frequency of mEPSCs on mutant FS interneurons compared with controls, indicative of a reduced number of excitatory synapses, but no changes in their amplitude (Fig. 3, A to E). We also found that the density of vesicular glutamate transporter type 1 (VGlut1^{+}) terminals contacting the soma of FS interneurons lacking Er81 is also reduced compared with

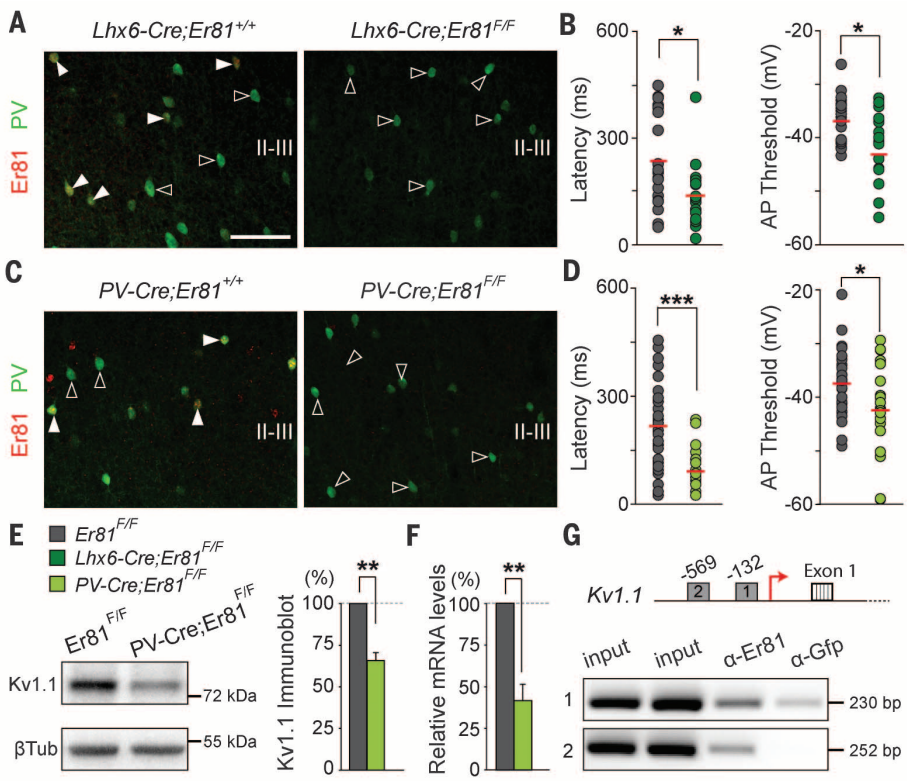

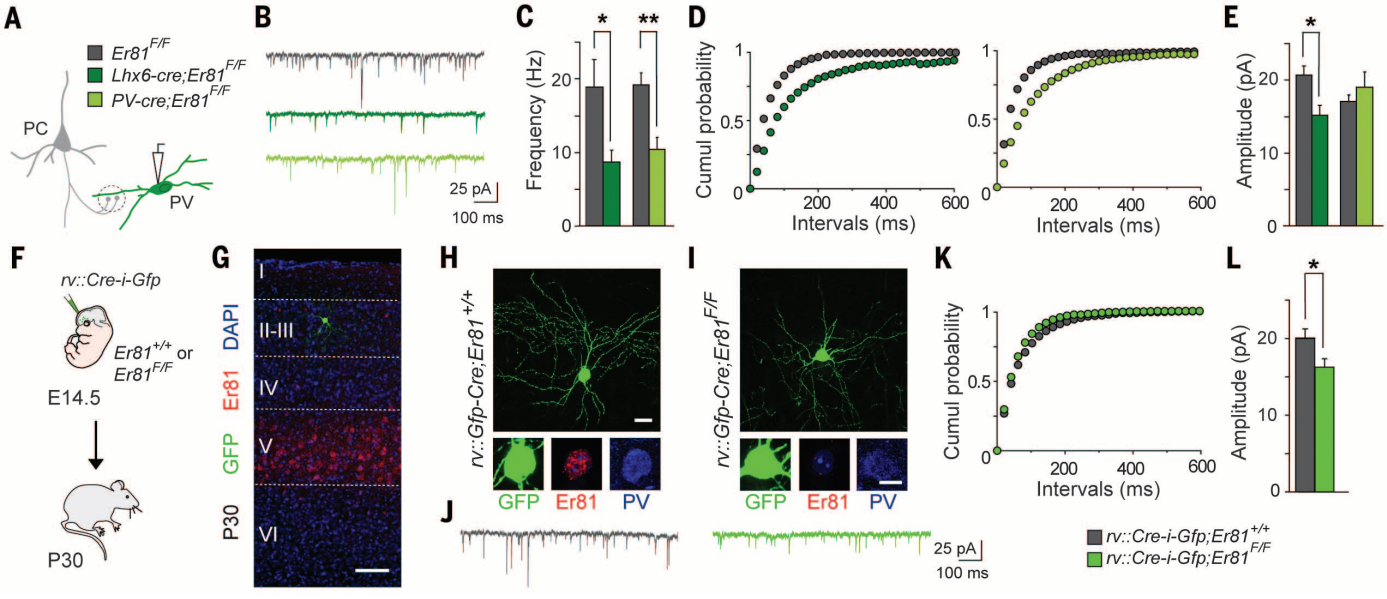

Fig. 2. Er81 regulates intrinsic properties of PV^{+} interneurons and Kv1.1 expression. (**A**) Normal distribution of PV^{+} interneurons in P30 layer II-III after embryonic genetic deletion of *Er81*. (**B**) Latency to the first spike and threshold potential for spike are significantly reduced in *Lhx6-Cre;Er81* conditional mutants (n = 20 and 18 cells, respectively; $P < 0.05$ for both values). (**C**) Normal distribution of PV^{+} interneurons in P60 layer II-III after postnatal genetic deletion of *Er81*. (**D**) Latency to the first spike and threshold potential for spike is significantly reduced in *PV-Cre;Er81* conditional mutants (n = 29 and 20 cells, respectively; $P < 0.001$ and $P < 0.05$, respectively). (**E**) Representative immunoblots (left) and quantification (right) of Kv1.1 protein in the cortex of control and conditional mutant mice (n = 5, $P < 0.01$). (**F**) Kv1.1 mRNA levels in PV^{+} interneurons isolated through FACS in control and conditional mutant mice (n = 4, $P < 0.01$). (**G**) ChIP assays on cortical tissue showing Er81 binding to Kv1.1 promoter regions (n = 3; $P < 0.05$ for site 2). Scale bar, 100 μm (A) and (C). Graphs represent means ± SEM.

Fig. 3. Reduced excitatory inputs onto PV interneurons in conditional *Er81* mutants. (**A**) Schematic of mEPSCs recordings in PV^{+} interneurons. (**B**) Representative traces. (**C** and **D**) Measurement and cumulative plot of mEPSC frequencies in *Lhx6-Cre;Er81*$^{F/F}$ (n = 11 and 9 cells, respectively; $P < 0.05$) and *PV-Cre;Er81*$^{F/F}$ (n = 17 and 10 cells, respectively; $P < 0.01$) mutants. (**E**) Measurement of mEPSC amplitudes in *Lhx6-Cre;Er81*$^{F/F}$ (n = 11 and 9 cells, respectively; $P < 0.05$) and *PV-Cre;Er81*$^{F/F}$ mutants (n = 17 and 10 cells, respectively; $P = 0.06$). (**F**) Experimental design for the labeling of sparse control and *Er81* mutant MGE-derived interneurons. (**G**) Labeled interneurons are sparsely distributed throughout the cerebral cortex at very low density. (**H** and **I**) Representative images of layer II-III PV^{+} interneurons after viral infection in the MGE. (**J**) Representative traces of mEPSCs from control and *Er81* mutant interneurons. (**K**) Cumulative plot of mEPSCs frequencies (n = 10 and 11 cells, respectively; $P = 0.45$). (**L**) Measurement of mEPSC amplitudes (n = 10 and 11 cells, respectively; $P < 0.05$). Scale bars, 10 μm and 5 μm (G) and (H) and 100 μm (I). Graphs represent means ± SEM.

controls (fig. S7, A and B), whereas the probability of release of these terminals is comparable for controls and mutants (fig. S7C). By contrast, recordings of mIPSCs from FS interneurons revealed a strong increase in their frequency without changes in amplitude in *PV-Cre;Er81$^{F/F}$;RCE* mice compared with controls (fig. S8, A to D). This increase likely reveals an increase in the number of presynaptic inhibitory contacts received by FS interneurons in the absence of Er81, because no changes were observed in γ-aminobutyric acid (GABA) release probability (fig. S8E).

The observed changes in the inputs received by FS interneurons in *Er81* conditional mutants have two possible explanations. One possibility is that Er81 directly regulates the connectivity of delay-type FS interneurons, as has been suggested for primary sensory neurons (*22*). Alternatively, the changes observed in conditional *Er81* mutants may reflect homeostatic adaptations in response to the loss of delay-type FS interneurons from cortical networks. To distinguish between these two possibilities, we ablated *Er81* from sparse cortical FS interneurons in each mouse. We used ultrasound imaging to inject low-titer retroviruses encoding *Cre* and *Gfp* into the MGE of wild-type and *Er81$^{F/F}$* embryos on embryonic day 14.5 (E14.5) (Fig. 3F), when FS interneurons are being generated. These experiments labeled very few interneurons that migrate to layer II-III in both genotypes and that lack Er81 expression only in *Er81$^{F/F}$* mice (Fig. 3, G to I). We then performed whole-cell recordings from layer II GFP$^+$ cells in P30 acute slices obtained from these mice. We found an almost complete loss of delay-type FS interneurons in the absence of Er81, as evidenced by a prominent reduction in the mean latency to the first spike and the levels of Kv1.1 expression in FS interneurons lacking Er81 compared with control cells (fig. S9, A to E). In contrast to these changes in intrinsic properties, we did not find

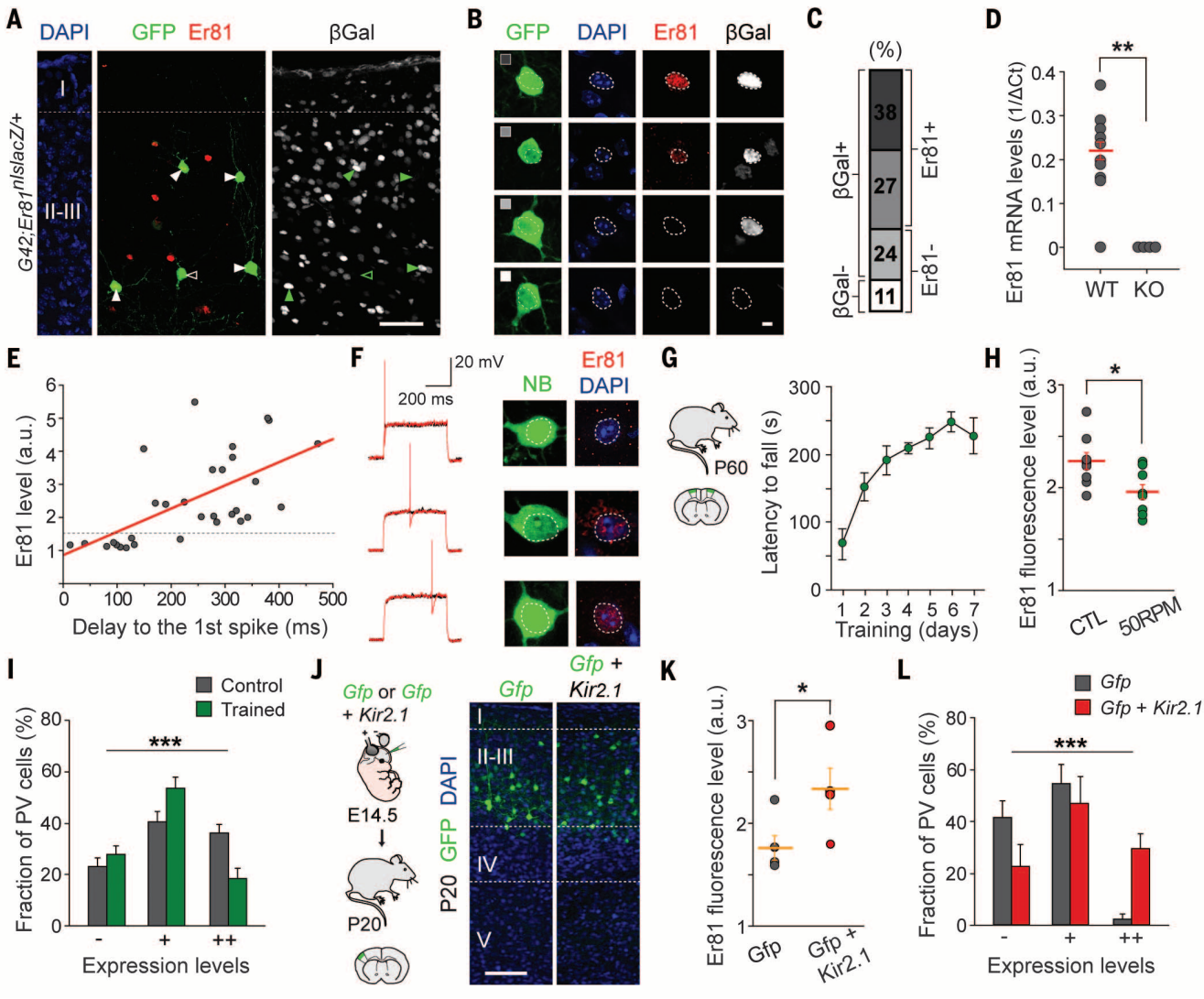

Fig. 4. Activity-dependent changes in Er81 expression. (**A**) Expression of Er81 and beta-galactosidase (βGal) in layer II-III PV$^+$ interneurons. (**B** and **C**) Representative examples and relative proportion of four groups of layer II-III PV$^+$ interneurons based on Er81 and βGal expression. (**D**) Most PV$^+$ interneurons contain significant Er81 mRNA levels. (**E**) Scatter plot of Er81 expression and latency to the first spike. Line, linear regression fit (R^2) = 0.63 ($P < 0.0001$). (**F**) Representative traces of recorded PV$^+$ interneurons illustrating the positive correlation between delayed firing and Er81 expression. (**G**) Learning curve (RotaRod performance) for motor task. (**H**) Er81 fluorescence intensity levels in PV$^+$ interneurons from control and trained animals ($n = 8$; $P < 0.05$). (**I**) Distribution of Er81 fluorescence intensities in layer II PV$^+$ interneurons from control and trained mice ($n = 8$; $P < 0.001$). Cells were grouped into three main classes on the basis of their levels of fluorescence intensity for nuclear Er81, < 1.3 times background levels (−), 1.3 to 1.6 times background (+), and > 1.6 times background levels (++). (**J**) Experimental design and distribution of electroporated pyramidal cells in layer II-III. (**K**) Mean Er81 fluorescence intensity in PV$^+$ interneurons from control and *Kir2.1*-electroporated mice ($n = 4$; $P < 0.01$). (**L**) Distribution of Er81 fluorescence intensities in layer III PV$^+$ interneurons from control and *Kir2.1*-electroporated mice ($n = 4$; $P < 0.001$), groups as in (I). Scale bars, 50 μm (A), 5 μm (B), and 100 μm (J). Graphs represent means ± SEM.

differences in the frequency of mEPSCs (Fig. 3, J to L) or the density of VGlut1$^+$ terminals contacting the soma of FS interneurons lacking Er81 compared with controls cells (fig. S9, F and G).

Our results demonstrate that Er81 generates cell diversity within FS basket cells in the mouse cortex. Because Er81 function is also required for the maintenance of delay-type FS interneurons in the adult cortex (as revealed by the analysis of *PV-Cre;Er81$^{F/F}$;RCE* mice), we next wondered when Er81 expression begins to distinguish both populations of interneurons. We used mice in which *nLacZ* have been inserted in the coding region of *Er81* (*Er81$^{nlsLacZ/+}$*) (*22*) and analyzed the fraction of FS interneurons expressing β-galactosidase in layer II-III of the somatosensory cortex. The large majority of layer II-III PV$^+$ interneurons contained β-galactosidase in the adult cortex, including many cells with undetectable levels of nuclear Er81 protein (Fig. 4, A to C). This surprising result suggests that almost all FS interneurons transcribe *Er81* mRNA. Alternatively, because β-galactosidase is known to perdure long after being synthesized (*23*), this result may indicate that the majority of FS interneurons may have transcribed *Er81* at some point during development. To distinguish between these two possibilities, we performed whole-cell patch-clamp recordings in PV$^+$ interneurons from layers II-III of the adult somatosensory cortex and subsequently collected the cytoplasm for single-cell reverse transcriptase PCR of *Er81*. Compared with *Er81* mutant interneurons (used to calibrate background), nearly all FS basket cells in the adult layer II-III of the somatosensory cortex contained substantial and comparable levels of *Er81* mRNA (10 out of 11 cells) (Fig. 4D), which suggests that the expression of Er81 in these interneurons is regulated post-transcriptionally. In addition, we found a direct correlation between the levels of nuclear Er81 protein and the latency to the first spike at near-threshold potential in FS interneurons (Fig. 4, E and F).

These observations prompted us to investigate whether the relative proportion of delay-type and nondelay-type FS interneurons remains constant in the adult cortex. Er81 transcription and activity is modulated by activity-dependent changes in intracellular calcium (*24*, *25*), which raises the possibility that the complement of layer II-III FS interneuron subtypes might be adjusted in response to variations in network activity (*26*, *27*). To test this hypothesis, we pharmacologically modified network activity levels in acute cortical slices. KCl or kainate rapidly decreased the relative proportion of layer II-III Er81$^+$ FS interneurons within 2 hours (fig. S10, A and B). This reduction in Er81$^+$ interneurons was associated with a parallel decrease in the mean latency to the first spike (fig. S10C). By contrast, pharmacological reduction of network activity with the L-type calcium channel blocker Nifedipine led to a significant rise in the proportion of Er81$^+$ FS interneurons and a concomitant increase in the mean latency to the first spike of these cells (fig. S10, D to F).

To characterize the activity-dependent regulation of Er81 expression in more physiological conditions, we trained mice in a motor-learning paradigm and analyzed the levels of Er81 expression in layer II of the motor cortex (Fig. 4G). Motor learning significantly decreased the proportion of Er81$^+$ FS interneurons compared with controls, because of a shift in Er81 levels toward lower intensity values (Fig. 4, H and I). To decrease the overall levels of activity in layer II-III pyramidal cells, we introduced the inward-rectifier potassium ion channel Kir2.1 in their cortical progenitor cells by means of in utero electroporation (*28*, *29*) and examined the levels of Er81 protein in layer III of the somatosensory cortex in adult mice (Fig. 4J). We found a prominent increase in the proportion of Er81$^+$ FS interneurons compared with controls, due to a change in Er81 levels toward higher-intensity values (Fig. 4, K and L). It was interesting that we did not observe comparable changes in other layers of the cortex, which suggests that this type of cellular plasticity mediated by Er81 might be limited to cortical layer II-III (fig. S11).

Our findings provide a mechanistic explanation for the activity-dependent regulation of interneuron properties through the transcriptional control of neuronal excitability and the modulation of synaptic inputs. Er81 has been previously shown to regulate the terminal differentiation of dopaminergic neurons and cerebellar granule cells (*30, 31*). In the cortex, Er81 shapes information processing by modulating the intrinsic properties of FS interneurons through the regulation of the Kv1.1 channel subunit, the expression of which is necessary for delayed firing (*21*). Other factors are likely involved in this process, because loss of Er81 does not completely transform fast-spiking interneurons into nondelayed cells. Kv1.1 function is also regulated by ErbB4 (*32*), a tyrosine kinase receptor that is highly expressed in the postsynaptic density of glutamatergic synapses contacting FS basket cells (*33*). This delineates a possible pathway through which synaptic activity may control Er81 expression to modulate the intrinsic properties of FS basket cells.

Our results also support the notion that activity-dependent mechanisms play a prominent role in the specification of neuronal properties (*34*, *35*). However, in contrast to the classical view in which the "specification" typically refers to the process by which cells achieve and maintain a stable fate independent of environment, our results suggest that layer II-III fast spiking basket cells may not exist as distinct classes of interneurons, but rather as a continuum of interneurons with "tunable" characteristics that adapt to the changing environment. The observation that cortical circuits reversibly adapt to changing levels of activity by tuning the efficacy of delayed firing within the population of FS basket cells suggests a novel mechanism of network plasticity, and reinforces the notion that interneuron function is ultimately context dependent (*5*).

Recent work has linked different configurations of FS basket cells, as revealed by distinct levels of PV expression, with learning and memory (*7*). Our analysis of *Er81* conditional mutant mice indicate that drastic imbalances in network configuration are accompanied by population-driven changes in structural synaptic plasticity, through which FS basket cells may lose their ability to filter out relatively weak, asynchronous stimulus.

REFERENCES AND NOTES

1. J. A. Cardin *et al*., *Nature* **459**, 663–667 (2009).
2. V. S. Sohal, F. Zhang, O. Yizhar, K. Deisseroth, *Nature* **459**, 698–702 (2009).
3. O. Yizhar *et al*., *Nature* **477**, 171–178 (2011).
4. J. Courtin *et al*., *Nature* **505**, 92–96 (2014).
5. H. Hu, J. Gan, P. Jonas, *Science* **345**, 1255263 (2014).
6. Y. Yazaki-Sugiyama, S. Kang, H. Câteau, T. Fukai, T. K. Hensch, *Nature* **462**, 218–221 (2009).
7. F. Donato, S. B. Rompani, P. Caroni, *Nature* **504**, 272–276 (2013).
8. S. J. Kuhlman *et al*., *Nature* **501**, 543–546 (2013).
9. S. B. Wolff *et al*., *Nature* **509**, 453–458 (2014).
10. C. P. Wonders, S. A. Anderson, *Nat. Rev. Neurosci.* **7**, 687–696 (2006).
11. N. Flames *et al*., *J. Neurosci.* **27**, 9682–9695 (2007).
12. R. F. Hevner *et al*., *Dev. Neurosci.* **25**, 139–151 (2003).
13. G. A. Ascoli *et al*., *Nat. Rev. Neurosci.* **9**, 557–568 (2008).
14. B. Rudy, C. J. McBain, *Trends Neurosci.* **24**, 517–526 (2001).
15. A. Gupta, Y. Wang, H. Markram, *Science* **287**, 273–278 (2000).
16. J. Helm, G. Akgul, L. P. Wollmuth, *J. Neurophysiol.* **109**, 1600–1613 (2013).
17. A. Woodruff, Q. Xu, S. A. Anderson, R. Yuste, *Front. Neural Circuits* **3**, 15 (2009).
18. M. Fogarty *et al*., *J. Neurosci.* **27**, 10935–10946 (2007).
19. T. D. Patel *et al*., *Neuron* **38**, 403–416 (2003).
20. S. Hippenmeyer *et al*., *PLOS Biol.* **3**, e159 (2005).
21. E. M. Goldberg *et al*., *Neuron* **58**, 387–400 (2008).
22. S. Arber, D. R. Ladle, J. H. Lin, E. Frank, T. M. Jessell, *Cell* **101**, 485–498 (2000).
23. M. I. Arnone, I. J. Dmochowski, C. Gache, *Methods Cell Biol.* **74**, 621–652 (2004).
24. J. W. Cave *et al*., *J. Neurosci.* **30**, 4717–4724 (2010).
25. H. Abe, M. Okazawa, S. Nakanishi, *Proc. Natl. Acad. Sci. U.S.A.* **108**, 12497–12502 (2011).
26. P. Li, M. M. Huntsman, *Neuroscience* **265**, 60–71 (2014).
27. E. Campanac *et al*., *Neuron* **77**, 712–722 (2013).
28. L. Cancedda, H. Fiumelli, K. Chen, M. M. Poo, *J. Neurosci.* **27**, 5224–5235 (2007).
29. M. Xue, B. V. Atallah, M. Scanziani, *Nature* **511**, 596–600 (2014).
30. N. Flames, O. Hobert, *Nature* **458**, 885–889 (2009).
31. H. Abe, M. Okazawa, S. Nakanishi, *Proc. Natl. Acad. Sci. U.S.A.* **109**, 8734–8739 (2012).
32. K.-X. Li *et al*., *Nat. Neurosci.* **15**, 267–273 (2012).
33. P. Fazzari *et al*., *Nature* **464**, 1376–1380 (2010).
34. L. N. Borodinsky *et al*., *Nature* **429**, 523–530 (2004).
35. I. Spiegel *et al*., *Cell* **157**, 1216–1229 (2014).

ACKNOWLEDGMENTS

We thank M. Fernández and C. Serra for excellent technical assistance; T. Gil and A. Dopplapudi for lab support; C. García-Frigola for help with ChIP experiments; T. Jessell for antibodies; and S. Arber, Z. J. Huang, and K. Nave for reagents and mouse lines. We are grateful to J. Burrone, N. Flames, C. Houart, M. Maravall, and B. Rico for critical reading of the manuscript, and members of the Marín and Rico laboratories for stimulating discussions and ideas. The data presented in this paper are tabulated in the supplementary materials. This work was supported by grants from the Spanish Ministry of Science and Innovation (SAF2011-28845), the European Research Council (ERC-2011-AdG 293683), and the Wellcome Trust (103714MA) to O.M. N.D. and L.L. were supported by EMBO postdoctoral fellowships. O.M. is a Wellcome Trust Investigator.

SUPPLEMENTARY MATERIALS

www.sciencemag.org/content/349/6253/1216/suppl/DC1
Materials and Methods
Figs. S1 to S13
References (*36*–*42*)

15 April 2015; accepted 6 August 2015
10.1126/science.aab3415